Simulation of 3D overtopping flow–object–structure interaction with a calibration-based wave generation method with DualSPHysics and SWASH

Suzuki, Tomohiro; García-Feal, Orlando; Domínguez, José M.; Altomare, Corrado

DOI
10.1007/s40571-022-00468-8

Publication date
2022

Document Version
Final published version

Published in
Computational Particle Mechanics

Citation (APA)
Suzuki, T., García-Feal, O., Domínguez, J. M., & Altomare, C. (2022). Simulation of 3D overtopping flow–object–structure interaction with a calibration-based wave generation method with DualSPHysics and SWASH. *Computational Particle Mechanics*, *9*(5), 1003-1015. https://doi.org/10.1007/s40571-022-00468-8

Computational Particle Mechanics (2022) 9:1003–1015
https://doi.org/10.1007/s40571-022-00468-8

Simulation of 3D overtopping flow–object–structure interaction with a calibration-based wave generation method with DualSPHysics and SWASH

Tomohiro Suzuki[1,2] · Orlando García-Feal[3] · José M. Domínguez[3] · Corrado Altomare[4]

Received: 10 July 2021 / Revised: 9 February 2022 / Accepted: 11 February 2022 / Published online: 14 March 2022

Abstract
Ongoing climate change is a significant threat to coastal communities. To understand potential risks during extreme storm events, detailed post-overtopping processes are investigated using DualSPHysics and SWASH with a newly developed approach. It is a calibrated-based wave generation: a target incident wave is first obtained from the validated SWASH model, and DualSPHysics creates the target incident wave by adjusting the offshore wave and bathymetry conditions. This one-way coupling process makes the DualSPHysics computation efficient enough to apply 3D simulation. With a vertical wall at the end of a room located at the end of the promenade in a mild and shallow foreshore, the present model shows a good correspondence on the wave force with the literature. After confirming the efficiency and accuracy of the present model, the 3D simulation with furniture inside the room was conducted and visualized with the state-of-the-art visualization technique. Based on the visualization, the potential risks during the extreme storm event are further discussed in this paper. The present work shows a further capability of DualSPHysics to deal with wave–object–structure interaction based on the latest developments in an efficient way. The developed model can be further used to understand the potential risks of ongoing climate change.

Keywords Wave–object–structure interaction · Wave generation · Calibration · Wave overtopping · SWASH · DualSPHysics

1 Introduction

Wave overtopping is one of the most significant concerns in urbanized coastal communities since it increases the risk for the people's safety and damages properties and urban assets. It is expected that such risks will be increased due to the ongoing Sea Level Rise [1, 2]. Further understanding of post-overtopping processes (e.g. overtopping discharges, overtopping volumes, flow depth, flow velocity, drag forces) will help to optimize people's safety and properties [3, 4].

However, detailed post-overtopping processes on a promenade/dike located in mild and shallow foreshores are not fully understood yet due to limited study cases. Shallow foreshore refers to shallow water conditions at the toe of the dike with a foreshore before it causing heavy wave breaking [5]. Limited information is available on the relationship of post-overtopping processes such as average overtopping discharge, overtopping volume, flow depth and velocity for mild and shallow foreshore conditions, even in EurOtop [6], one of the most used overtopping manuals in Europe. The bound infragravity waves are transformed into free long

✉ Tomohiro Suzuki
tomohiro.suzuki@mow.vlaanderen.be

Orlando García-Feal
orlando@uvigo.es

José M. Domínguez
jmdominguez@uvigo.es

Corrado Altomare
corrado.altomare@upc.edu

[1] Flanders Hydraulics Research, Berchemlei 115, 2140 Antwerp, Belgium

[2] Faculty of Civil Engineering and Geosciences, Delft University of Technology, Stevinweg 1, 2628 CN Delft, The Netherlands

[3] EPHYSLAB Environmental Physics Laboratory, CIM-UVIGO, Universidade de Vigo, Campus As Lagoas, 32004 Ourense, Spain

[4] Maritime Engineering Laboratory, Department of Civil and Environmental Engineering, Universitat Politecnica de Catalunya-BarcelonaTech (UPC), 08034 Barcelona, Spain

waves in shallow foreshores and influence the overtopping processes significantly [7, 8]. Neglecting infragravity waves, the process on the shallow foreshore will not be accurately represented. The flow behaviour on the dike in shallow foreshores is not the same as in the deepwater cases in the existing studies [9]. Among the limited study, it has to be highlighted that Stansby et al. [10] predicted overtopping volumes for solitary waves with Boussinesq/shallow water, SPH and VOF modelling. Hunt-Raby et al. [11] provide well-defined data on overtopping flow based on the solitary and focussed wave. These would be a good validation data set for the further study of overtopping flow.

One of the difficulties in the study of flow properties on the dike is velocity measurement. Overtopping flow is typically thin and repeats in wet and dry conditions during the overtopping event. Therefore, it is not easy to measure flow velocity accurately in physical models and field measurements. In many cases, the flow velocity is measured using two wave gauges. Apart from the tip and individual wave propagation velocity (by tracking crests/through), no flow velocity information can be measured. This problem does not occur in numerical modelling due to its nature: one can output all detailed hydraulic and hydrodynamic properties in numerical models at any region of the defined numerical domain. In addition to the need for modelling wave–structure interaction [12], it is now well documented that waterborne debris is also responsible for increased damage [13] and needs to be modelled. In order to obtain detailed information on wave–structure–objects interaction, mesh-based and mesh-less methods are being used for coastal engineering practices. Recent studies show good capabilities of smoothed particle hydrodynamics (SPH) models to deal with wave–objects interaction [13, 14] and even debris flows by expanding the SPH method with a distributed-contact discrete element method (DCDEM) [15] and with project Chrono [16]. Such numerical models are helpful to understand post-overtopping processes where overtopping flow, objects (e.g. debris) and structure interaction is essential. However, they need a large domain due to the (very) long foreshore when it is applied to the mild and shallow foreshores. In addition, wave–object–structure interaction is a 3D problem, hence requiring even higher computational resources.

Recently, Suzuki et al. [17] investigated the risk on the dike/promenade in mild and shallow foreshore by means of SWASH [18], which is based on the nonlinear shallow water equation with non-hydrostatic pressure term. The computation is not expensive compared to CFD models, but is similar to Boussinesq models [19, 20]. It allowed us to understand overall overtopping wave–structure interaction in 2DV, yet the work was limited to simple bathymetry configurations due to the nature of a depth-integrated model (e.g. not possible to calculate the effect of the ceiling of a room).

Coupling models is useful to overcome the shortcomings of both models [21]. On the one hand, wave propagation is calculated by such depth-integrated models (e.g. SWASH, Boussinesq models [22]), and on the other hand, the detailed run-up and wave–structure interaction are solved by high-end numerical models (e.g. OpenFOAM [23], DualSPHysics [24–26]). With regard to coupling models in SPH, Altomare et al. [27] first introduced the multi-layered piston concept to couple SWASH and DualSPHysics [28]. It is a one-way coupling method in which the velocity field calculated with SWASH is passed to DualSPHysics at a specific coupling location by means of a moving boundary. The information from SWASH is interpolated along the water depth to assign the horizontal component of the orbital velocity at each boundary particle, depending on its z-coordinate. Further coupling techniques based on DualSPHysics were developed in recent years. For example, Altomare et al. [29] introduced improved relaxation zone method. In this method, the movement of the fluid particles is controlled by correcting their orbital motion based on a weighting function in a specified generation area. Verbrugghe et al. [30] developed a two-way coupling method for wave propagation and wave–structure interaction in a deep water condition based on open boundary conditions (i.e. inflow/outflow). However, none of the model is fully applicable or validated for simulating wave overtopping in mild and shallow foreshores when the coupling point comes to very/extremely shallow water—e.g. at or close to the toe of the dike. The limitation of those models for generating waves at the toe are related to the high nonlinearity in very shallow water and limited volume of the water mass in the DualSPHysics domain. Using open boundaries in DualSPHysics [31] for nonlinear wave generation [32] can be a good option. However, the method is not yet validated for such highly nonlinear waves at a very shallow (or even dry) coupling point including reflection from the dike. Usui et al. [33] developed a theoretical paddle movement to generate an arbitrary wave shape in a wave flume, but it is only applicable to a flat bottom profile. Similarly, a development of a theoretical paddle movement might be possible, but it will not be easy due to the fact that the wave transformation is highly nonlinear in the shallow/dry zone.

In order to overcome the issues shown above, a novel calibration-based wave generation method was developed in this study as an alternative. It enables to simulate the post-overtopping processes of an individual wave on the dike/promenade in mild and shallow foreshores efficiently. The technique is helpful to calculate wave–structure interactions. For example, the maximum wave force estimation acting on a coastal structure can be obtained based on the present method. Also, it can be applied to understand wave–object interaction in 3D.

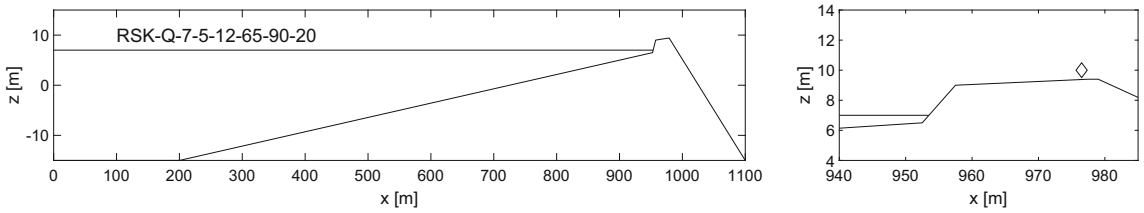

Fig. 1 Overview of the shallow foreshore and dike (left panel) and zoom of the promenade area (right panel). The diamond marker indicates the position of the output point of unobstructed flow depth and velocity

The paper is structured as follows. First, the methods used in the paper are explained in Sect. 2. Next, in Sect. 3, the calibration is conducted for the present study cases. In Sect. 4, the post-overtopping processes of the 3D overtopping flow–object–structure interaction in an apartment on a dike in a mild and shallow foreshore are simulated based on the calibrated paddle movement. The simulated results are analysed and visualized to understand better the state-of-the-art visualization technique in the 3D environment [34]. The calibration method, computational cost and potential risks of the post-overtopping processes are discussed further in Sect. 5.

2 Methods

2.1 DualSPHysics

The numerical model used for this study is DualSPHysics. See detailed governing equation and numerical techniques in [28]. This paper used a newly developed boundary condition, the modified dynamic boundary condition (hereafter mDBC; [35]). The typically used boundary conditions in DualSPHysics, DBC [36], become too repulsive in dry-to-wet conditions and complex pre-processing techniques are needed to reduce the gap created between fluid and structure/bathymetry [37]. Without mDBC, this gap makes the simulation of bore propagation on the promenade interacting with free objects less straightforward. On top of using mDBC, the coupling of DualSPHysics and Chrono-Engine [38] is used for modelling the object–object interaction [39]. Canelas et al. [39] validated the fluid–structure–structure model based on physical experiments. With this method, the collisions of furniture/structure are properly modelled. The second novelty in DualSPHysics formulation used in this work is the density diffusion term (DDT) by Fourtakas et al. [40]. This stabilization mechanism improves the density field and allows for long simulations.

2.2 Calibration-based wave generation method

In this study, post-overtopping processes in an apartment room situated at the end of the promenade in a mild and shallow foreshore are simulated with DualSPHysics based on the *calibration-based wave generation method*.

As a first step, the target wave needs to be created with an available resource, for example, a computationally less expensive numerical wave model or a physical model. In this study, wave transformation in a shallow foreshore and overtopping over a dike with a promenade in 2DV were simulated in SWASH (Fig. 1). It generates the time series of incident (i.e. unobstructed) flow depth and velocity at a target point, see the diamond maker in Fig. 1. It is noted that the SWASH simulations applied to this study correspond to the cases from [17]: no calculation was conducted for this study (except preliminary testing cases to get incident wave condition at the coupling point, see details in 3.1), but the time series of free surface and velocity of existing calculations are extracted. These time series are treated as target incident waves for DualSPHysics simulation. As a second step, the target wave needs to be reproduced by a numerical model. It is noted that the numerical model needs to be capable of dealing with wave–structure–object interaction. In this study, DualSPHysics is selected since it is possible of dealing with wave–structure–object interaction without extra calculations (i.e. objects can be calculated as a cluster of particles, which directly interact with fluid particles within DualSPHysics). Calibration is an iterative process, and thus, tests are repeated until a satisfactory result is obtained. In the DualSPHysics model, waves are generated as a movement of a piston as a standard method [41, 42], and therefore, the paddle movement together with the water level is modified during the calibration. When the target wave time series at the specified location is reproduced, the calibration process is completed. In our case, the target is the time series of overtopping discharge q, which is derived from a product of the flow depth and horizontal flow velocity at the end of the promenade. It is noted that only horizontal flow is relevant in our case since it is shallow water flow.

2.3 Data selection

According to Suzuki et al. [17], the average overtopping discharge q and maximum individual overtopping volumes Vmax had a strong relationship; therefore, simulating an

Table 1 Selected cases and overtopping flow properties during the maximum overtopping event. Numbers used in the case name are properties of the test condition. See details in Suzuki et al. [17]

Case	Class	Actual average q (l/s/m)	Vmax (l/m)	h_{max} (m)	u_{max} (m/s)
RSK_Q_7_4_12_65_95_20	1 l/s/m	0.7	1799	0.21	3.6
RSK_Q_7_5_12_65_90_20	10 l/s/m	10	7123	0.35	5.8
RSK_Q_8_4_12_69_90_20	100 l/s/m	89	19,037	0.74	7.4

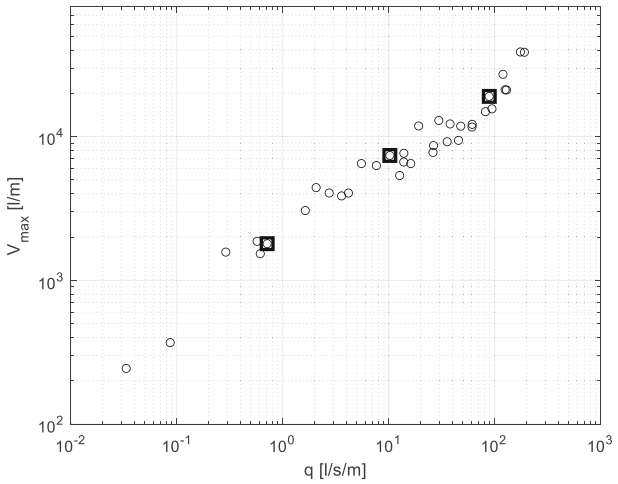

Fig. 2 Vmax and q for the selected wave overtopping cases and entire data from Suzuki et al. [17]

individual overtopping flow in the time window Vmax can represent a maximum overtopping event during 1000 waves of a specific class of average overtopping discharge.

In this study, three cases from three classes of the overtopping discharge are selected to simulate the post-overtopping processes, namely '1 l/s/m', '10 l/s/m' and '100 l/s/m', see Table 1. As can be seen in the table, the actual overtopping discharges selected were not precisely the same as the name of the classes, but they are close enough to represent these overtopping discharges, see the scatters of the Vmax for different q in Fig. 2. The time series of water surface elevations and velocities in the maximum wave overtopping event in the selected cases are shown in Fig. 3. These are used as inputs for the calibration of incident waves at the end of the promenade. They will be reproduced in DualSPHysics and the calibrated paddle motion in 2DV, which are used to simulate the post-overtopping event in a room of an apartment building located at the end of the promenade in 3D.

2.4 Model settings

Once the target waves are obtained from the SWASH modelling, calibration is conducted using DualSPHysics in 2DV. The calibration aims to obtain a proper wave paddle motion

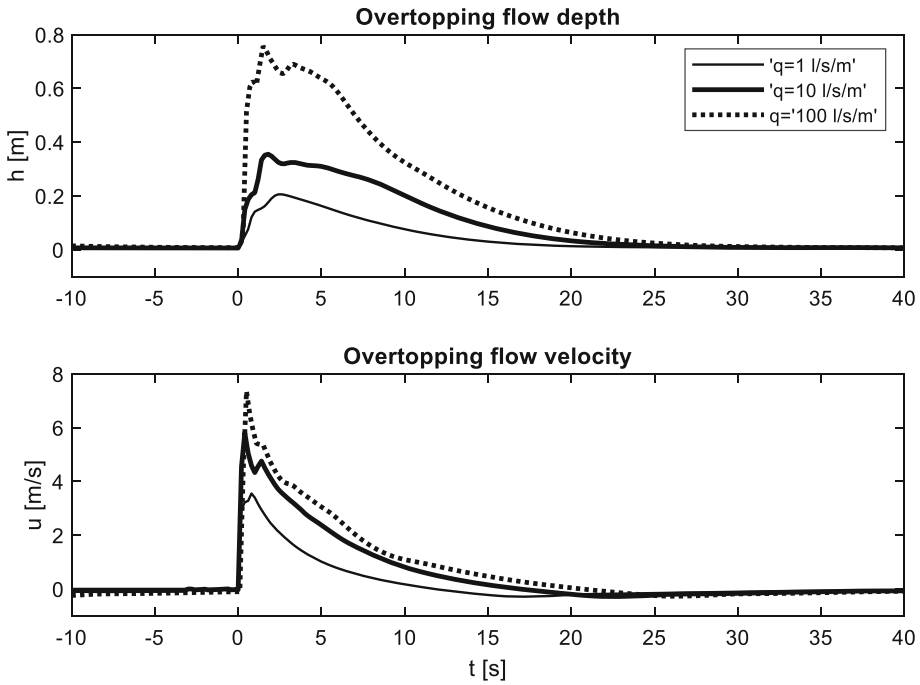

Fig. 3 Time series of water surface elevations and velocities measured at the end of the promenade during the maximum overtopping event in the selected wave overtopping cases

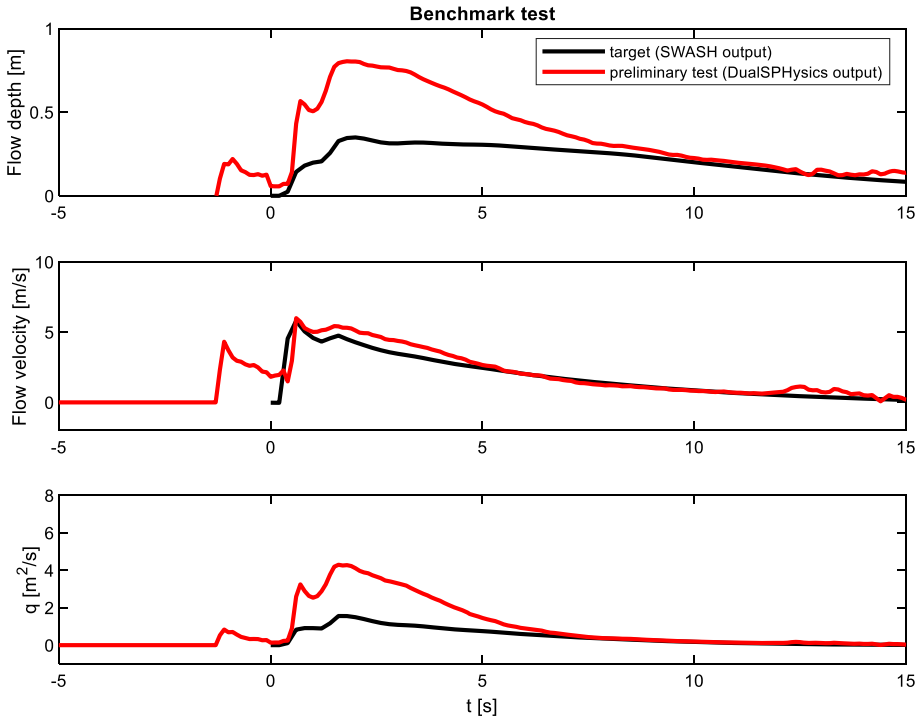

Fig. 4 Time series of flow depth (upper panel), velocity (middle panel) and q (lower panel) for the preliminary test and target

that generates target incident overtopping flow at the specified location. The distance between the toe and the initial paddle position should not be too long to keep the computational time short enough. In our work, the wave paddle was placed 27 m away from the toe of the dike (which corresponds to 12% of offshore wavelength). In our calibration, the promenade and dike slope were set the same as in reality. The toe depth was selected deeper than the reality to keep the necessary amount of water (Vmax and water mass not passing to the overtopping measurement point) in a limited calculation domain, while the depth is kept constant for the wave generation (Fig. 5). The input parameter for the calibration is the depth at the toe (i.e. SWL) and the paddle motion (i.e. paddle position in time). For the simplicity of the calibration process, the piston was not ML piston (multi-layered piston [27]), but just a single wave board. Otherwise, the paddle movement for each layer needs to be calibrated, which makes the calibration process much more complicated without benefit, especially for shallow foreshore conditions, in which the velocity profile is almost uniform.

The parameters/settings used in the DualSPHysics simulations are as follows. Coefficient to calculate the smoothing length, Coefh is 1.5 as suggested in [43], density diffusion term DDT is [40] with value 0.1, and artificial viscosity is 0.01. In order to have some bottom friction effect, multiplication factor of viscosity value with boundary, viscoboundfactor 2 is used [44]. The initial interparticle distance, Dp are 0.025, 0.04, 0.05 m, for 1 l/s/m, 10 l/s/m and 100 l/s/m, respectively.

3 Calibration

3.1 Preliminary testing

Before starting the calibration, the coupling method of [45] was applied to check whether the coupling method works for the case of 10 l/s/m when the coupling point is very shallow. For this test, one-layered paddle motion was obtained from SWASH incident wave simulation (i.e. the bathymetry is flattened at the coupling point, see details in [45]) by integrating the time series of the velocity at the fixed location (i.e. 27 m away from the toe of the dike) and it was applied to the piston in DualSPHysics model. Figure 4 shows the flow depth, velocity and q of this preliminary test. As shown in the figure, the flow depth is highly overestimated. The error can be generated because of four possible reasons: (1) the paddle motion is based on the velocity measured at the fixed point, while in reality, the paddle position is moved in time (i.e. velocity at the actual position of the paddle at each moment will be necessary), (2) the paddle reached the toe of the dike during the generation, and thus, water between the dike and the paddle was squeezed and eventually gives higher water surface elevation at the promenade, (3) the actual water surface elevation at the moment of the initial time step (i.e. snapshot at the domain between the paddle and overtopping point in the SWASH modelling) is not constant, and (4) the time window which has to be used for the coupling is unknown a priori. Minor differences can lead to different consequences. For this reason, it is unsure that inlet/outlet [32] can be directly used

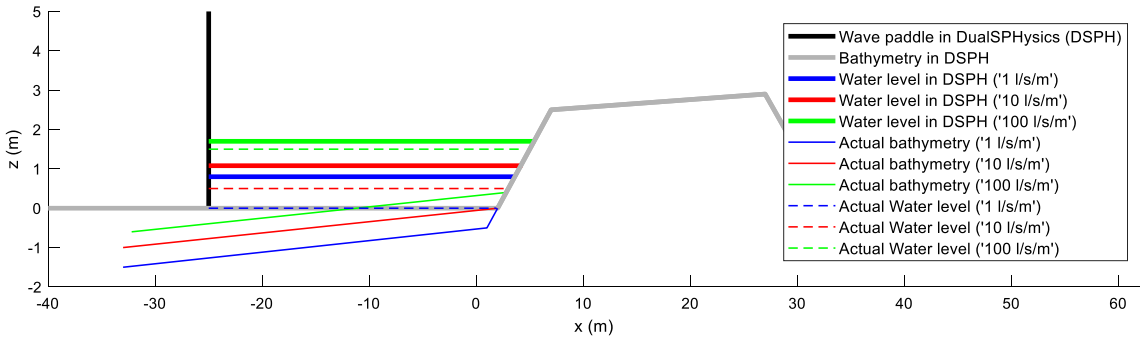

Fig. 5 Bathymetry, initial paddle position of the wave paddle and water levels in DualSPHysics modelling (water levels are ones from successful calibration, and actual bathymetries and water levels used in SWASH modelling [17]; all relative levels based on the crest of the dike)

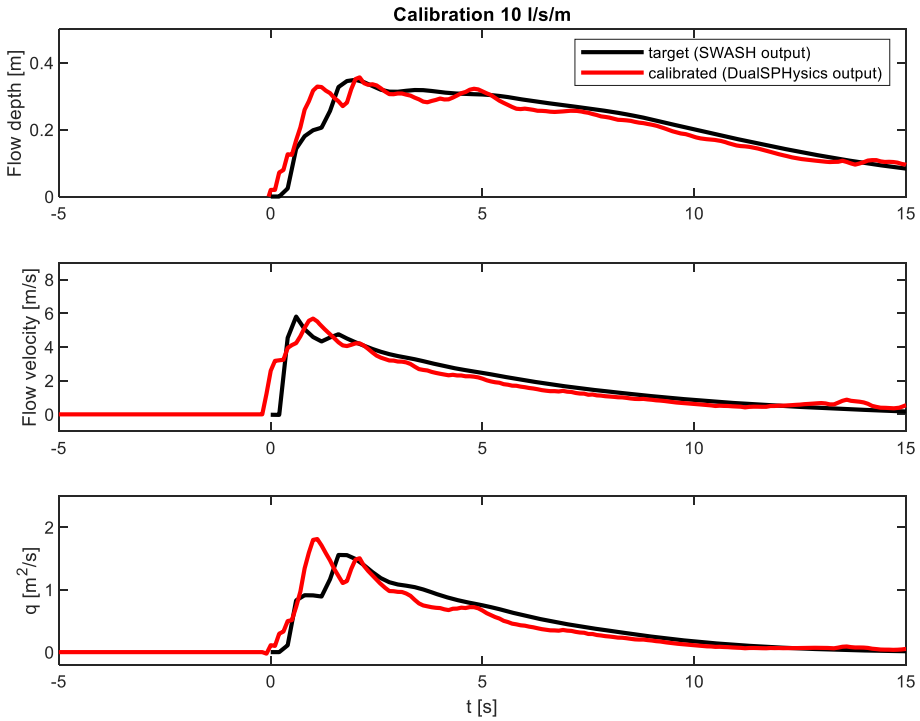

Fig. 6 Calibrated flow depth, velocity and q for 10 l/s/m case

to obtain a good result, and therefore, the coupling method is not further explored in this study.

3.2 Calibration results

The paddle motion and water level were first calibrated for the 10 l/s/m case, by tuning the paddle velocity and the initial water level (Fig. 5). The first trial reduced the velocity of the paddle movement used in the last section, which gave higher flow depth. At the same time, the water level was increased to generate the wave with a limited stroke of the paddle. After some iterations, a good incident wave was obtained, see Fig. 6. This case matches the target time series of the water surface elevation and the velocity from SWASH. The time series of instantaneous q is also following the target curve. After the target paddle movement was obtained for the case 10 l/s/m, two extra cases, namely the 1 l/s/m and 100 l/s/m were also calibrated. On this occasion, the same paddle movement was used, but only the different water levels are tested for the calibration since these are in the same overtopping regime (i.e. overtopping over a dike with a promenade in a shallow foreshore) and give similar overtopping patterns as shown in Fig. 3. As shown in Fig. 7, the results show a good agreement with this approach. The calibration results suggest that the water level change is a crucial aspect since the volume of water in the domain affects different overtopping volumes in the studied regime. By changing the water level, the volume of water inside the model domain is decided, while the shape of the overtopping was well maintained by the paddle movement calibrated for the 10 l/s/m case.

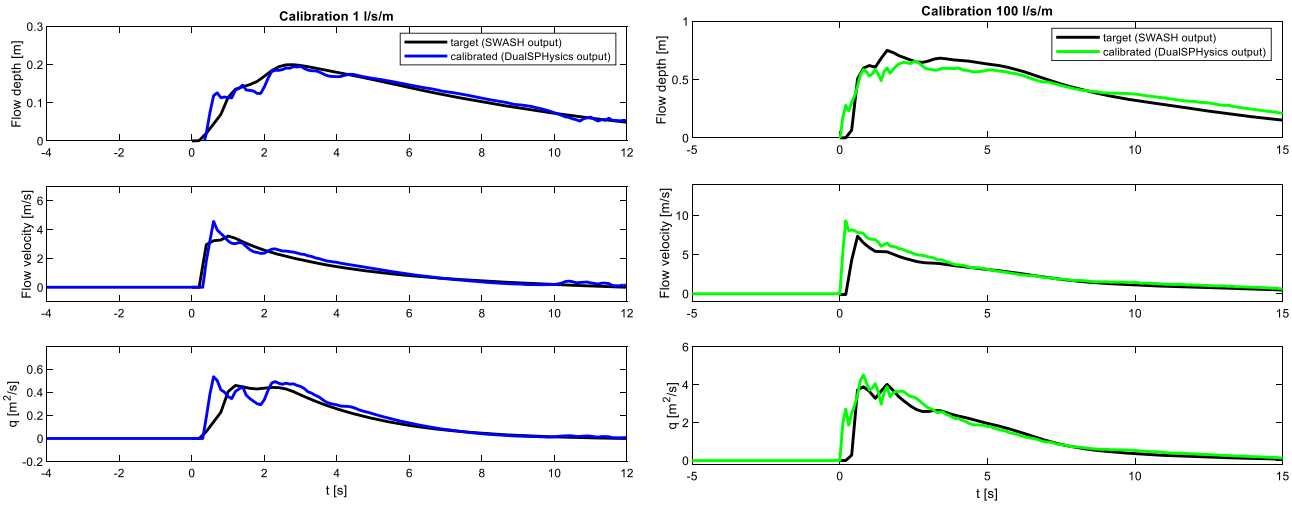

Fig. 7 Calibrated flow depth, velocity and q for 1 l/s/m and 100 l/s/m case

In order to evaluate the overall performance of the executed calibration, Willmott's refined index of agreement dr is applied to the time series of q here, following the evaluation method in Gruwez et al. [23]. The dr can be calculated based on MAE (mean absolute error) and MAD (mean absolute deviation), ranging from -1 to 1. It gives 0.72, 0.71 and 0.80, respectively, for 1 l/s/m, 10 l/s/m and 100 l/s/m. They fall into 'Good' and 'Very Good' defined by [23]. It is recommended that the calibration be more than 0.7 so that the calibrated time series represents the target time series.

Note that the DualSPHysics calculations for the calibration were not time-consuming: the computational time for one run was 7 min using GeForce RTX 2080 Ti.

4 Modelling of wave–object–structure interaction

4.1 Model schematization

Based on the calibrated paddle motion and water levels, 2DV wave–structure interaction and 3D wave–object–structure interaction are modelled. 2DV wave–structure interaction is based on an extended bathymetry with an apartment room at the end of the promenade to see water surface elevation and force acting on the room's back wall. 3D wave–object–structure interaction modelling included some furniture in the room on top of the extended bathymetry in 3D. The furniture is not a fixed object, but can be freely moved when critical forces are exerted on it. See the schematization in Fig. 8. The furniture modelled in this simulation are a sofa, a coffee table and a TV with a cabinet. The furniture was reproduced by a cluster of particles which represent the geometry of each object extracted from STL files. The density of all the furniture is set the same, 700 kg/m^3, for simplicity. Note that the aim is not to perform a strict validation of the movement of specific items of furniture. The interparticle distance of the furniture was the same as the one for fluid. The smallest object (the coffee table) has dimensions of $0.8 \times 0.8 \times 0.45$ m, and the largest object (the sofa) measures approx. $2.3 \times 1.1 \times 0.85$ m. The maximum water level is 0.3 m in 10 l/s/m case (dp $= 0.04$ m), and thus, around 8 particles covered the depth. Canelas et al. [39] demonstrated that the DVI models show a good representation of the motion of the object even with the lowest resolution $H/\mathrm{dp} = 3$.

In these simulations, it is assumed that the apartment windows have already broken, and thus, there is no obstruction at the entrance of the room. See example calculations of window failure in Chen et al. [46]. It indicates that the window's strength is a function of the configuration and location of the window.

4.2 Force estimation with the calibration method

The 2DV simulation is very similar to the physical model case of Chen et al. [47], namely with a shallow foreshore and a dike with a promenade. At the end of the promenade, a high vertical wall is situated. The measurement of the force acting on the wall is available. In this section, the validity of the numerical model of the present study is investigated using the physical model test results. The input of the force estimation from Chen et al. [47] is relatively simple. It links the force to the maximum wave run-up height on a vertical wall. The force is estimated with the equation below.

$$F = 0.33\rho g h^2 \tag{1}$$

where F is force, ρ the water density, g the gravitational acceleration and h the wave run-up height.

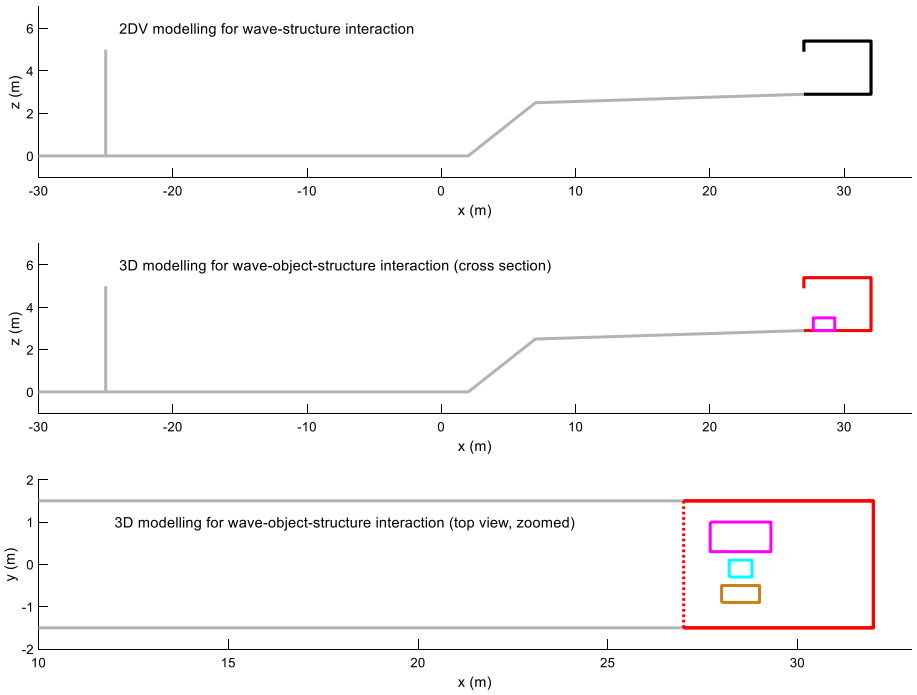

Fig. 8 Schematization of 2DV and 3D modelling

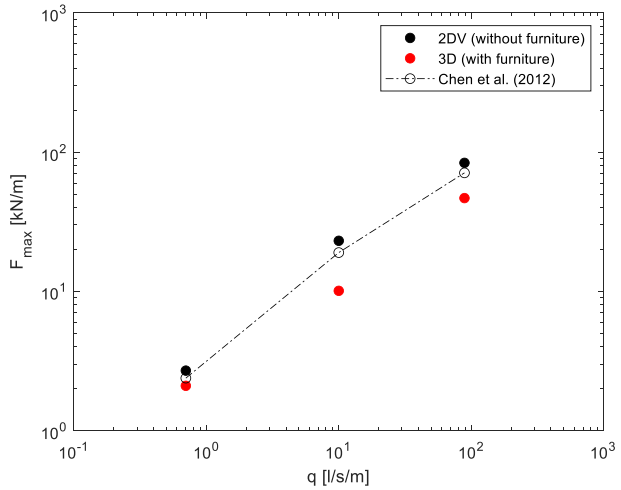

Fig. 9 Maximum force acting on the back wall of the room with different overtopping discharge

In order to have the wave run-up value on each modelling of the present study (i.e. 1 l/s/m, 10 l/s/m and 100 l/s/m), one extra numerical simulation was conducted, which is 100 l/s/m case. In this case, the wave run-up is interrupted by the ceiling of the room, and therefore, the wave run-up value is not valid in the existing case. To obtain the wave run-up value, the room configuration was replaced with a high wall (i.e. no overtopping and no ceiling). For 1 l/s/m and 10 l/s/m cases, wave run-up is not reached the ceiling, and thus, the wave run-up values are directly obtained in the existing models.

Figure 9 (black dots) shows the maximum force measured in the 2DV without furniture and force estimation based on Chen et al. [47]. The differences between the DualSPHysics simulation and Chen's estimation of 1 l/s/m, 10 l/s/m and 100 l/s/m are 12, 21 and 17%, respectively. It is noted that a range of 20% error can be considered acceptable for wave impact cases, according to Altomare et al. [48]. From this result, it can be concluded that the estimated forcing on the vertical back wall by DualSPHyics is valid in practice. Even though the other physical parameters such as water surface elevations and velocity simulated in the present model are not validated here, we assume that the model represents these properly.

Figure 9 (red dots) shows the maximum force measured in 3D with furniture. In this case, the force acting on the back wall is reduced due to the obstruction of the furniture. It is a different behaviour compared to Wüthrich et al. [49], which shows that the debris can increase the force on the structure. The structural shape can partly explain this: the present study used a closed room while Wüthrich et al. [49] used the building with openings (i.e. the building consists of pillars and beams). In the present model, the incoming bore first hit the furniture, and the momentum of the bore is slightly reduced. Then consequently, the bore containing the furniture hit the wall. The process is visualized with the state-of-the-art visualization technique in the next section.

4.3 Visualization of wave–object–structure interaction

In order to understand the post-overtopping process better, the 3D wave–object–structure simulation is visualized

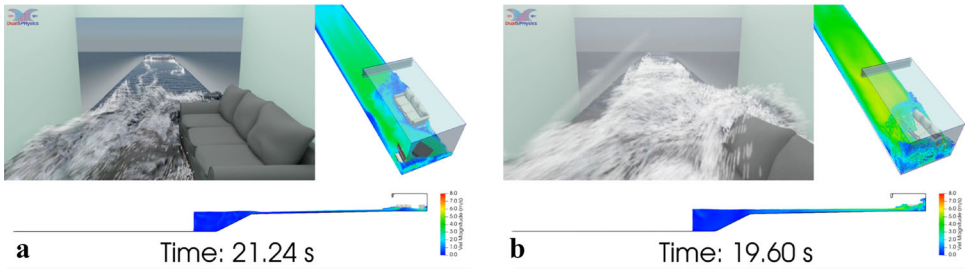

Fig. 10 Snapshot of overtopping event **a** 1 l/s/m: furniture are moved except sofa and **b** 10 l/s/m: all the furniture are moved

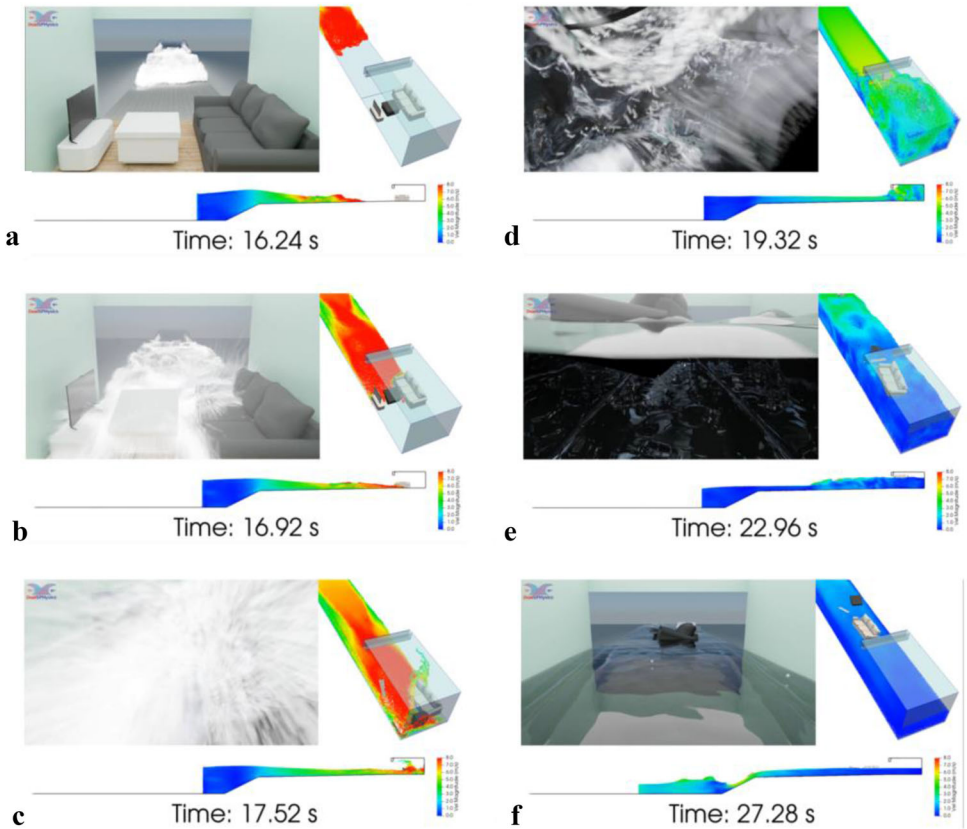

Fig. 11 Snapshot of overtopping event 100 l/s/m: **a** bore propagating on the promenade, **b** bore is interacting with furniture, **c** furniture hit to the wall at the end of the room, **d** the room is filled with water, **e** reflected wave brings the furniture to offshore, **f** one object reached the dike slope

with the state-of-the-art visualization technique [34]. Such detailed visualization provides an opportunity for professionals, the general public and possible stakeholders to understand the post-overtopping event qualitatively. It helps discuss the overtopping risks and possible measures for the countermeasures (e.g. evacuation strategies). The three videos cover a wide range of overtopping events, from 1 to 100 l/s/m. To the authors' knowledge, it is the first time to visualize such different levels of the overtopping events in a comprehensive way. Note that the eyepoint of the 3D image is 1.60 m from the bottom, assuming a person of 1.70–1.75 m tall.

Figure 10 shows snapshots of the overtopping events of 1 and 10 l/s/m. Most of the furniture (except sofa: a few cm drift) is moved by the bore during the overtopping event 1 l/s/m. 10 l/s/m case makes all the furniture moved. Figure 11 shows snapshots of the overtopping event of the case 100 l/s/m. As seen in the figure, the overtopping wave is quite energetic in this case: the bore can move all the furniture and make them hit the wall behind. Even though the incident flow depth is around 0.7 m, when it is combined with the bore propagation velocity, furniture obstruction and wave reflection at the wall behind, the highest water level goes up to the ceiling filling most of the room with water (see Fig. 11d). Note that the cross-sectional view at the bottom figure represents the highest water level in the whole width in practice (whole domain in y-direction since it is like a side view of wave flume with a certain width), and therefore, the water level is not that high for entire y-direction. The water level in the y-direction is not uniform due to the 3D effect induced by

Table 2 Difference of number of particles and simulation time for traditional method and calibration method (assuming dp = 0.05 m and the domain is from the case of Suzuki et al. [17])

Method	Model	Order of magnitude of number of particles	Real time to be simulated (s)	Simulation time
Traditional method	Full simulation in 3D and 1000 waves	370 million	12,000	Not tested
Calibration method	Simulation in 2DV and target time window	0.03 million	40	7 min
	Full simulation in 3D and target time window	1.2 million	40	8 h

the furniture (if there is no furniture, then the wave remains uniform in the *y*-direction).

As a result of realistic visualization, it is now recognizable how violent is the overtopping waves for different overtopping discharges. The videos are available as Supplementary Information.

5 Discussions

5.1 Calibration method

The quality of the calibration method is decided by the quality of the input data (either numerical model or physical model) and numerical models which calculate the wave–object–structure interaction. Therefore, the selection of the models is essential. On top of that, the calibration quality also influences the result. It is recommended to calibrate the model until dr $\geq$ 0.7 is obtained to maintain the quality of the method. It is noted that the input model SWASH in this study has been well validated for the wave transformation and overtopping over dikes and individual overtopping volume with the shallow foreshores configuration [18, 50]. The DualSPHysics model has also been validated well for wave–structure interactions, as stated earlier.

It is underlined that the calibration method is feasible for the combination of two numerical models, as shown in this study, and for a combination of a physical model and a numerical model. For example, the incident wave obtained from a physical model can be reproduced with the calibration method. In contrast to a coupling of two numerical models, physical models cannot provide all the velocity and water surface elevation in time at the coupling point. Therefore, calibration is an excellent alternative to reproduce a target wave.

During the calibration, quick visualization will help to reduce the number of trials. For example, visualization will help to understand at what moment the paddle needs to be accelerated.

In the calibration process in this study, it was necessary not only to calibrate the paddle movements but also to modify the bathymetry to adjust to the wave generation system in DualSPHysics, and to change the water levels. It is arbitrary, but in turn, it shows different calibration possibilities. It is not confirmed in our study, but the calibration can be completed only by changing with paddle displacement without any water level change. One can explore this possibility with a fixed water level. However, due to the high nonlinearity of the wave propagation on the dry impermeable structure, it is helpful to keep the possibility that the water level can be changed. Eventually, it increases the possibility to obtain the desired wave at the target point. Further optimization might be useful when a more efficient method is necessary.

5.2 Computational cost

Based on our experience, the first calibration takes more time (e.g. 10 times try and error), but the second one will be faster. It is because one starts to know how the change of the movement of the paddle affects the water surface elevation. It is very similar to calibration of incident wave in physical modellings—calibration is typically accelerated as cases are increased. As mentioned earlier, good results were obtained based on Willmott's refined index for different overtopping discharge cases only by changing the water levels.

As noted earlier, one run in our simulation took 7 min (~ 0.03 million fluid particles and the time window of 40 s), and the 3D simulation with furniture took 10 h in the case of 100 l/s/m (dp = 0.05 m). Both were simulated with GeForce RTX 2080 Ti. In total, the simulation time is minimal compared to the conventional method, which models the whole domain and entire time window (i.e. 1000 wave periods for wave force estimation). See Table 2 for the comparison. As can be seen, the traditional method is not feasible with DualSPHysics, in practice. The computational cost and the memory used for the simulation can also be saved by limiting the domain using the calibration method.

5.3 Discussion on overtopping risks

As shown in the 3D simulation, the furniture can be moved by the overtopping bore. Even though the total force acting on the wall is reduced due to the obstruction of the flow by the furniture in this configuration, such furniture movement is an extra risk factor for people. The velocity of the furniture measured in the simulation goes up to 5 m/s. In the worst-case scenario, people might be pressed between furniture and wall. The pressure of the corner of the furniture can be extremely high accidentally (e.g. large mass furniture move fast heading with the corner). It is a great threat for people inside the building. No wonder people are already evacuated in such a situation, but it is useful that any numerical model can predict such physics. The other phenomenon that deserves to be studied is that one piece of furniture (the TV shelf) goes offshore due to the return flow within 10 s after the bore hitting in the 100 l/s/m case. As indicated in Suzuki et al. [17], reflected wave from the back wall is one of the additional risks for the overtopping waves for human stability, but return flow drawing to the sea will be another potential risk for people's safety. According to [17], the negative velocity reach 3 m/s for their 15 l/s/m case. One benefit of the numerical model is to be used to communicate such different risks with local communities—dissemination of scientific knowledge is an important topic for disaster prevention/evaluation. It can be better achieved by the state-of-the-art visualization technique, as stated earlier.

6 Conclusions

In the present work, a calibration-based wave generated method is proposed and applied to 3D overtopping flow–object–structure interaction. As for the target wave input for the calibration method, three cases from Suzuki et al. [17] are selected, which have links to average overtopping discharges with different orders of magnitude (i.e. 1 l/s/m, 10 l/s/m and 100 l/s/m). It is noted that these inputs were calculated using SWASH, which was already validated on the overtopping cases under shallow foreshore conditions in the literature. As preliminary testing, a selected time series of the horizontal velocity extracted from the incident wave run in SWASH was applied to obtain the target wave time series at the target point, following the coupling methodology of Altomare et al. [27]. However, the obtained results do not match the target wave time series mainly because the coupling point is very shallow. See details of the difficulties in Sect. 3.1. After that, we tested the calibration-based wave generation method. The method needs some iterations changing the input paddle movement and water levels until the target wave is obtained. Following some try and error, we obtained the acceptable target wave time series with a limited error in h, u and q, for all three cases. The calibrated paddle movements and water levels are first applied to the 2DV simulations without furniture. Based on Chen et al. [47], the force calculation using the calibration method is validated. The result indicates that the calculated force acting on the back wall is within the expected range. After this confirmation, the model is further applied to the 3D configuration with furniture. With furniture, the measured wave force acting on the back wall is slightly reduced due to the momentum lost during the interaction between the incoming bore and the furniture. The process is confirmed with the state-of-the-art visualization technique. It provides much qualitative information on the post-overtopping processes of the overtopping wave, making it possible to discuss further the risks of the overtopping wave hitting a room with furniture.

The present work not only confirms the accuracy and the efficiency of the proposed calibration method, but also shows the usefulness of the state-of-the-art visualization technique. The calibration method is also applicable to physical model input, theoretically. The computational cost is much reduced, as shown in Table 2, owing to the efficient methodology proposed in the present study, and thus, it is possible to apply the present methodology to wave–object–structure interaction in 3D configuration. It reduced the number of the particle to 1/300 (i.e. 370 to 1.2 million) and the computational time window to 1/300 (i.e. 12,000 s to 40 s) in our case. Wave–object interaction can relatively easily be modelled in DualSPHysics since the model deals with the floating object as a cluster of particles. Based on the visualization, further potential risks are also detected.

In conclusion, the present work shows the capability of DualSPHysics to deal with complex interactions (e.g. wave–object–structure interactions) using the latest developments with the proposed calibration method. It is an essential step for coastal engineering to understand additional risks and develop countermeasures against ongoing climate change.

Acknowledgements This research was partially funded by Xunta de Galicia (Spain) under the project ED431C 2017/64 'Programa de Consolidación e Estructuración de Unidades de Investigación Competitivas (Grupos de Referencia Competitiva)' cofunded by European Regional Development Fund (ERDF). Dr. José M. Domínguez acknowledges funding from Spanish government under the programme 'Juan de la Cierva-incorporación 2017' (IJCI-2017-32592). A part of the research was conducted during the CREST (Climate REsilient CoaST) project (http://www.crestproject.be/en), funded by the Flemish Agency for Innovation by Science and Technology, grant number 150028.

Availability of data and materials Three videos ('1 l/s/m' = Composed_1L.mp4, '10 l/s/m' = Composed_10L.mp4 and '100 l/s/m' = Composed_100L.mp4) are available as supplementary material.

Declarations

Conflict of interest The authors declare that they have no conflict of interest.

References

1. Weisse R, von Storch H, Niemeyer HD, Knaack H (2012) Changing north sea storm surge climate: an increasing hazard? Ocean Coast Manag 68:58–68. https://doi.org/10.1016/j.ocecoaman.2011.09.005
2. Neumann B, Vafeidis AT, Zimmermann J, Nicholls RJ (2015) Future coastal population growth and exposure to sea-level rise and coastal flooding—a global assessment. PLoS ONE 10:e0118571. https://doi.org/10.1371/journal.pone.0118571
3. Arrighi C, Oumeraci H, Castelli F (2017) Hydrodynamics of pedestrians' instability in floodwaters. Hydrol Earth Syst Sci 21:515–531. https://doi.org/10.5194/hess-21-515-2017
4. Bruce T, Sandoval C (2017) Wave overtopping hazard to pedestrians: video evidence from real accidents. In: Proceedings of the coasts, marine structures and breakwaters 2017, pp 501–512
5. Hofland B, Chen X, Altomare C, Oosterlo P (2017) Prediction formula for the spectral wave period T M-1,0 on mildly sloping shallow foreshores. Coast Eng Int J Coast Harb Offshore Eng 123:21–28
6. Van der Meer JW, Allsop NWH, Bruce T, De Rouck J, Kortenhaus A, Pullen T, Schüttrumpf H, Troch P, Zanuttigh B (2018) Manual on wave overtopping of sea defences and related structures. An overtopping manual largely based on European research, but for Worldwide application
7. Lashley CH, Bricker JD, van der Meer J, Altomare C, Suzuki T (2020) Relative magnitude of infragravity waves at coastal dikes with shallow foreshores: a prediction tool. J Waterw Port Coast Ocean Eng 146:04020034
8. Altomare C, Suzuki T, Chen X, Verwaest T, Kortenhaus A (2016) Wave overtopping of sea dikes with very shallow foreshores. Coast Eng 116:236–257
9. Altomare C, Gironella X, Suzuki T, Viccione G, Saponieri A (2020) Overtopping metrics and coastal safety: a case of study from the catalan coast. J Mar Sci Eng 8:556
10. Stansby PK, Xu R, Rogers BD, Hunt AC, Borthwick AGL, Taylor PH (2008) Modelling Tsunami overtopping of a sea defence by shallow-water boussinesq, VOF and SPH methods. CRC Press, Oxford, pp 255–261
11. Hunt-Raby AC, Borthwick AGL, Stansby PK, Taylor PH (2011) Experimental measurement of focused wave group and solitary wave overtopping. J Hydraul Res 49:450–464. https://doi.org/10.1080/00221686.2010.542616
12. Chen X, Hofland B, Altomare C, Suzuki T, Uijttewaal W (2015) Forces on a vertical wall on a dike crest due to overtopping flow. Coast Eng 95:94–104. https://doi.org/10.1016/j.coastaleng.2014.10.002
13. Domínguez JM, Crespo AJC, Hall M, Altomare C, Wu M, Stratigaki V, Troch P, Cappietti L, Gómez-Gesteira M (2019) SPH simulation of floating structures with moorings. Coast Eng 153:103560. https://doi.org/10.1016/j.coastaleng.2019.103560
14. Crespo AJC, Altomare C, Domínguez JM, González-Cao J, Gómez-Gesteira M (2017) Towards simulating floating offshore oscillating water column converters with smoothed particle hydrodynamics. Coast Eng 126:11–26. https://doi.org/10.1016/j.coastaleng.2017.05.001
15. Canelas RB, Domínguez JM, Crespo AJC, Gómez-Gesteira M, Ferreira RML (2017) Resolved simulation of a granular-fluid flow with a coupled SPH-DCDEM model. J Hydraul Eng 143:06017012. https://doi.org/10.1061/(asce)hy.1943-7900.0001331
16. Ruffini G, Briganti R, De Girolamo P, Stolle J, Ghiassi B, Castellino M (2021) Numerical modelling of flow-debris interaction during extreme hydrodynamic events with DualSPHysics-CHRONO. Appl Sci 11:3618. https://doi.org/10.3390/app11083618
17. Suzuki T, Altomare C, Yasuda T, Verwaest T (2020) Characterization of overtopping waves on sea dikes with gentle and shallow foreshores. J Mar Sci Eng 8:752. https://doi.org/10.3390/jmse8100752
18. Zijlema M, Stelling G, Smit P (2011) SWASH: an operational public domain code for simulating wave Fi elds and rapidly varied Fl ows in coastal waters. Coast Eng 58:992–1012. https://doi.org/10.1016/j.coastaleng.2011.05.015
19. Chen BQ, Kirby JT, Dalrymple RA, Kennedy AB (2000) Boussinesq modelling of wave transformation, breaking, and runup. II: 2D. J Waterw Port Coast Ocean Eng 126:48–56
20. Kennedy BAB, Chen Q, Kirby JT, Dalrymple RA (2000) Boussinesq modelling of wave transformation, breaking, and runup. I: 1D. J Waterw Port Coast Ocean Eng 126:39–47
21. Vacondio R, Altomare C, De Leffe M, Hu X, Le Touzé D, Lind S, Marongiu JC, Marrone S, Rogers BD, Souto-Iglesias A (2021) Grand challenges for smoothed particle hydrodynamics numerical schemes. Comput Part Mech 8:575–588. https://doi.org/10.1007/s40571-020-00354-1
22. Lashley CH, Zanuttigh B, Bricker JD, van der Meer J, Altomare C, Suzuki T, Roeber V, Oosterlo P (2020) Benchmarking of numerical models for wave overtopping at dikes with shallow mildly sloping foreshores: accuracy versus speed. Environ Model Softw 130:104740. https://doi.org/10.1016/j.envsoft.2020.104740
23. Gruwez V, Altomare C, Suzuki T, Streicher M, Cappietti L, Kortenhaus A, Troch P (2020) Validation of RANS modelling for wave interactions with sea dikes on shallow foreshores using a large-scale experimental dataset. J Mar Sci Eng 8:650. https://doi.org/10.3390/jmse8090650
24. Lowe RJ, Buckley ML, Altomare C, Rijnsdorp DP, Yao Y, Suzuki T, Bricker JD (2019) Numerical simulations of surf zone wave dynamics using smoothed particle hydrodynamics. Ocean Model 144:101481
25. González-Cao J, Altomare C, Crespo AJC, Domínguez JM, Gómez-Gesteira M, Kisacik D (2019) On the accuracy of dual-sphysics to assess violent collisions with coastal structures. Comput Fluids 179:604–612. https://doi.org/10.1016/j.compfluid.2018.11.021
26. Gruwez V, Altomare C, Suzuki T, Streicher M, Cappietti L, Kortenhaus A, Troch P (2020) An inter-model comparison for wave interactions with sea dikes on shallow foreshores. J Mar Sci Eng 8:985. https://doi.org/10.3390/jmse8120985
27. Altomare C, Domínguez JM, Crespo AJC, Suzuki T, Caceres I, Gómez-Gesteira M (2015) Hybridization of the wave propagation model SWASH and the meshfree particle method SPH for real coastal applications. Coast Eng J 57:1550024. https://doi.org/10.1142/S0578563415500242
28. Domínguez JM, Fourtakas G, Altomare C, Canelas RB, Tafuni A, García-Feal O, Martínez-Estévez I, Mokos A, Vacondio R, Crespo AJC et al (2021) DualSPHysics: from fluid dynamics to multiphysics problems. Comput Part Mech. https://doi.org/10.1007/s40571-021-00404-2
29. Altomare C, Taglia B, Dominguez JM, Suzuki T, Viccione G (2018) Improved relaxation zone method in SPH-based model for coastal engineering applications. Appl Ocean Res 81:15–33. https://doi.org/10.1016/j.apor.2018.09.013
30. Verbrugghe T, Domínguez JM, Crespo AJC, Altomare C, Stratigaki V, Troch P, Kortenhaus A (2018) Coupling methodology for smoothed particle hydrodynamics modelling of non-linear wave–structure interactions. Coast Eng 138:184–198. https://doi.org/10.1016/j.coastaleng.2018.04.021
31. Tafuni A, Domínguez JM, Vacondio R, Crespo AJC (2018) A versatile algorithm for the treatment of open boundary conditions in smoothed particle hydrodynamics GPU models. Comput Methods Appl Mech Eng 342:604–624. https://doi.org/10.1016/j.cma.2018.08.004

32. Verbrugghe T, Domínguez JM, Altomare C, Tafuni A, Vacondio R, Troch P, Kortenhaus A (2019) Non-linear wave generation and absorption using open boundaries within DualSPHysics. Comput Phys Commun 240:46–59. https://doi.org/10.1016/j.cpc.2019.02.003
33. Usui A, Aoki S, Kawasaki K, Suzuki T (2017) Construction of a theoretical model to realize arbitrary water level rise in a self-propelled waveguide channel. J Jpn Soc Civ Eng Ser B2 Coast Eng 73:1–6
34. García-Feal O, Crespo AJC, Gómez-Gesteira M (2021) Visual-SPHysics: advanced fluid visualization for SPH models. Comput Part Mech. https://doi.org/10.1007/s40571-020-00386-7
35. English A, Domínguez JM, Vacondio R, Crespo AJC, Stansby PK, Lind SJ, Chiapponi L, Gómez-Gesteira M (2021) Modified dynamic boundary conditions (MDBC) for general-purpose smoothed particle hydrodynamics (SPH): application to tank sloshing, dam break and fish pass problems. Comput Part Mech. https://doi.org/10.1007/s40571-021-00403-3
36. Crespo AJC, Gómez-Gesteira M, Dalrymple R (2007) Boundary conditions generated by dynamic particles in SPH methods. Comput Mater Contin 5:173–184
37. Zhang F, Crespo A, Altomare C, Domínguez J, Marzeddu A, Shang SP, Gómez-Gesteira M (2018) Dualsphysics: a numerical tool to simulate real breakwaters. J Hydrodyn 30:95–105. https://doi.org/10.1007/s42241-018-0010-0
38. Tasora A, Anitescu M (2011) A matrix-free cone complementarity approach for solving large-scale, nonsmooth, rigid body dynamics. Comput Methods Appl Mech Eng 200:439–453. https://doi.org/10.1016/j.cma.2010.06.030
39. Canelas RB, Brito M, Feal OG, Domínguez JM, Crespo AJC (2018) Extending DualSPHysics with a differential variational inequality: modeling fluid–mechanism interaction. Appl Ocean Res 76:88–97. https://doi.org/10.1016/j.apor.2018.04.015
40. Fourtakas G, Dominguez JM, Vacondio R, Rogers BD (2019) Local uniform stencil (LUST) boundary condition for arbitrary 3-D boundaries in parallel smoothed particle hydrodynamics (SPH) models. Comput Fluids 190:346–361. https://doi.org/10.1016/j.compfluid.2019.06.009
41. Altomare C, Domínguez JM, Crespo AJC, González-Cao J, Suzuki T, Gómez-Gesteira M, Troch P (2017) Long-crested wave generation and absorption for SPH-based DualSPHysics model. Coast Eng 127:37–54. https://doi.org/10.1016/j.coastaleng.2017.06.004
42. Domínguez JM, Altomare C, Gonzalez-Cao J, Lomonaco P (2019) Towards a more complete tool for coastal engineering: solitary wave generation, propagation and breaking in an SPH-based model. Coast Eng J 61:15–40. https://doi.org/10.1080/21664250.2018.1560682
43. Rota Roselli RA, Vernengo G, Altomare C, Brizzolara S, Bonfiglio L, Guercio R (2018) Ensuring numerical stability of wave propagation by tuning model parameters using genetic algorithms and response surface methods. Environ Model Softw 103:62–73. https://doi.org/10.1016/j.envsoft.2018.02.003
44. Barreiro A, Domínguez JM, Crespo AJC, González-Jorge H, Roca D, Gómez-Gesteira M (2014) Integration of UAV photogrammetry and SPH modelling of fluids to study runoff on real terrains. PLoS ONE 9:e111031. https://doi.org/10.1371/journal.pone.0111031
45. Altomare C, Domínguez JM, Crespo AJC, Suzuki T, Caceres I, Gómez-Gesteira M (2016) Hybridization of the wave propagation model SWASH and the meshfree particle method SPH for real coastal applications. Coast Eng J. https://doi.org/10.1142/S0578563415500242
46. Chen X, Jonkman SN, Pasterkamp S, Suzuki T, Altomare C (2017) Vulnerability of buildings on coastal dikes due to wave overtopping. Water 9:394. https://doi.org/10.3390/w9060394
47. Chen X, Hassan W, Uijttewaal W, Verwaest T, Verhagen HJ, Suzuki T, Jonkman SN (2012) Hydrodynamic load on the building caused by overtopping waves. In: Proceedings of the proceedings of the coastal engineering conference
48. Altomare C, Crespo AJ, Domínguez JM, Gómez-Gesteira M, Suzuki T, Verwaest T (2015) Applicability of smoothed particle hydrodynamics for estimation of sea wave impact on coastal structures. Coast Eng 96:1–12
49. Wüthrich D, Ylla Arbós C, Pfister M, Schleiss AJ (2020) Effect of Debris damming on wave-induced hydrodynamic loads against free-standing buildings with openings. J Waterw Port Coast Ocean Eng 146:04019036. https://doi.org/10.1061/(asce)ww.1943-5460.0000541
50. Suzuki T, Altomare C, Veale W, Verwaest T, Trouw K, Troch P, Zijlema M (2017) Efficient and robust wave overtopping estimation for impermeable coastal structures in shallow foreshores using SWASH. Coast Eng 122:108–123. https://doi.org/10.1016/j.coastaleng.2017.01.009